CHAPTER

4

Kinematic concepts in minimally invasive surgical flexible robotic manipulators: State of the art

Jiewen Lai[a], Bo Lu[b], and Hongliang Ren[a]

[a]Department of Electronic Engineering, The Chinese University of Hong Kong, Sha Tin, Hong Kong [b]Robotics and Microsystem Center, Soochow University, Suzhou, China

Introduction

Minimally invasive surgery (MIS) allows the surgeon to perform surgical operations through small incisions by administering the instruments inserted into the patient's body, thereby reducing the patient's wound healing time, associated pain and suffering, and risk of infection. The use of surgical robots in MIS has been enhancing the precision of the intraoperative MIS task and the dexterity of surgical instrument maneuvering. With the prevailing 5G technology, robot-assisted MIS surgery leads to the possibility of remote surgery [1]. Different types of MIS have been semi-robotized or robotized [2], such as surgery in ophthalmology [3], heart [4], thoracic [5], gastrointestinal [6], gynecology [7], orthopedics [8], etc. Even though many surgical robots are commercially available in the market, the development of novel surgical robots and medical mechatronic instruments that better fit specific medical procedures has continued in academia. Among all novel surgical robots, flexible robots, or soft/continuum robots [9], have stood out from the crowds of many other rigid-limbs robots in robot-assisted minimally invasive surgery and interventions (RAMIS) [10]—for their inherent compliance, dexterity, and safe human-robot interaction. State-of-the-art medical robots that employ flexible manipulators can be found in some big brands of commercial surgical robots, such as the Da Vinci SP platform [11], the SHURUI system [12], and the Medrobotics Flex Robotic System [13].

According to a recent metaanalysis [14], many interdisciplinary challenges of MIS flexible robotic manipulators have been tackled, such as robotic design, materials selection, fabrication, actuation methods, sensing, force exertion, modeling, and stiffness variability, among others. One of the most well-studied fields is the kinematics of these flexible continuum robots. Flexible robots for MIS kinematically distinguish themselves from conventional industrial robots in terms of reduced dimensions (therefore, the type of joints and transmission mechanisms vary), motion constraints, joint perceptions, geometry, use of materials, etc. The continuum structure of the manipulator body physically guarantees essential flexibility. In Ref. [15], the authors summarize continuum robot kinematics into two mappings, namely, robot-independent mapping and robot-dependent mapping. The former mapping exists independently from the actuation mechanism as it concerns only the task space and the configuration space of the robot, while the latter focuses on the relationship between the actuation mechanism and the geometrical resultant of the robot. Different actuation methods also constitute the variety in kinematics modeling [16]. These kinematics concepts are mostly applicable to the MIS flexible manipulators designed for surgical manipulation, endoscopic applications, and force sensing [9]. However, for the novel soft material-based flexible MIS robots, modification in kinematics shall be given with the consideration of including but not limited to the soft material's properties, hysteresis upon the actuation, mechanics, nonlinear deformation, and robot-environment interaction. All these factors diversify the kinematics concepts of MIS flexible robots. Alternatively, with the help of machine learning algorithms and robotic perception, the mappings can also be coupled and become data-driven [17], neglecting conventional kinematics.

Handbook of Robotic Surgery
https://doi.org/10.1016/B978-0-443-13271-1.00070-4

TABLE 1 Databases and the corresponding search entries.

Database	Search query syntaxes[a]
Web of Science (WOS)	TI = (soft OR continuum OR flexible) AND TI = (robot* OR manipulator*) AND TI = (surg* OR medic* OR MIS*) AND TI = (survey OR review OR advances OR overview)
Scopus	TITLE("Soft" OR "Continuum" OR "Flexible") AND TITLE("Robot*" OR "Manipulator*") AND TITLE("Surg*" OR "Medic*" OR "MIS*") AND TITLE("survey" OR "review" OR "overview")
PubMed	(("robot*"[All Fields]) AND ("soft"[title] OR "continuum"[title] OR "flexible"[title])) AND ("surg*"[Title] OR "MIS"[Title] OR "medic*" [Title]) AND ("survey"[All Fields] OR "review"[Title] OR "overview"[Title] OR "advances"[Title])

[a] *Filtered with the range of 2012–22.*

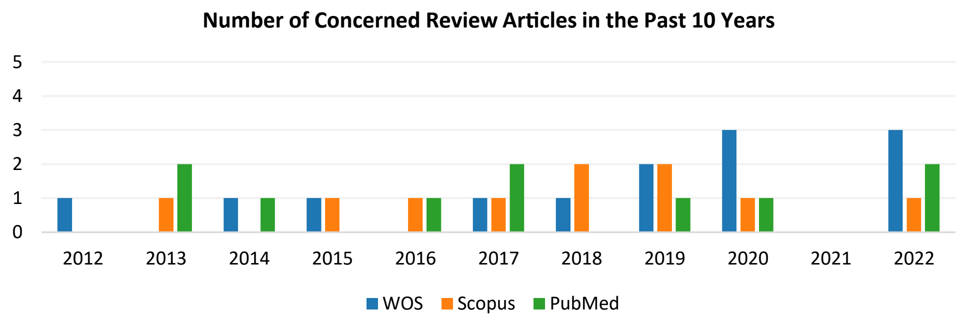

FIG. 1 Number of review articles on soft continuum robots for MIS in the past 10 years.

To exhaust the published review articles of the concerning fields, we searched the keywords on different databases. The databases and the corresponding search entries are given in Table 1, and the result is given in Fig. 1. Even though not many, recent decades of review articles on MIS-oriented (or other medical) flexible robots can be found in various scopes, such as medical applications [9,14,18,19], shape sensing techniques [20], specific surgeries and medical interventions [21,22], retrospectives and prospects [23,24], control strategies [25], etc. In-depth kinematic modeling surveys on soft continuum robots are available in the literature [15,26–29], focusing on the mathematical modeling of different kinds. However, there lacks a review of how the field utilizes the kinematics concepts in their MIS flexible robotic applications. The chapter herein introduces the kinematic concepts in MIS flexible robotic manipulators through case studies of the recent decade (2012–22). Typical state-of-the-art works are listed and compared regarding kinematics modeling and kinematic-based applications with minimally invasive surgical initiatives. By raising case studies, the kinematic concepts would have a stronger connection to medical considerations. The discussion is restricted to rigid-link continuum manipulators and soft manipulators designed for MIS or other similar medical applications—therefore, large robots are excluded from the case studies. The robots we discuss are referred to the manipulators with cylindrical or conical structures with an aspect ratio (length to cross-sectional diameter) greater than 1, and generally with 3D steerability that can be kinematically modeled. Note that concentric tube robots, dielectric elastomer actuators, and other uncommon soft robots are out of our scope.

The rest of this chapter is organized as follows: "Kinematic frameworks for MIS flexible manipulators" section briefly introduces the popular kinematics models for flexible robots—with the classification of rigid-link and soft manipulators. "Kinematics-based applications for MIS flexible robots" section demonstrates some kinematics-based applications for MIS robots through case studies. "Conclusions" section discusses the kinematics concepts in MIS flexible robots, and "Future scenario" section concludes this chapter.

Kinematic frameworks for MIS flexible manipulators

Since the MIS flexible robotic manipulators would be used in the confined intracavity and surgical site, where the sensing techniques may not always be available, developing a referable kinematic model would be a baseline for any tangible MIS robots. The investigation of the kinematics of MIS manipulators is the prerequisite of quasistatic robotic motion control and robotic automation control, such as trajectory following and motion control.

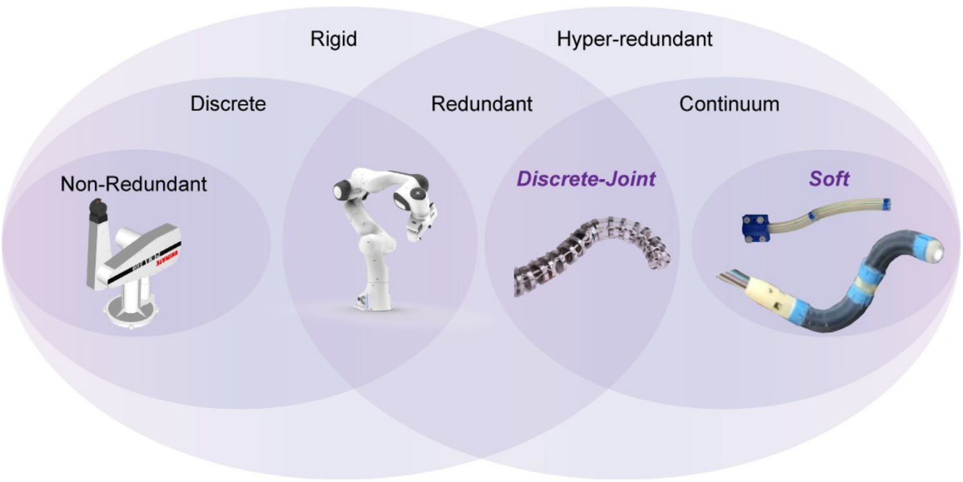

FIG. 2 Venn diagram of the rigid and hyperredundant robots based on the classification of materials of DOFs. The continuum robots can be further categorized as discrete-jointed and soft robots. (Images from left to right: 6-DOF PUMA 560, 7-DOF Franka Emika robot arm, an extensible segment tendon-driven continuum robot (Continuum Robotics Lab, University of Toronto), a cable-driven soft robot (Biomimetic Robotics Lab of PolyU), and the STIFF-FLOP soft medical robot.)

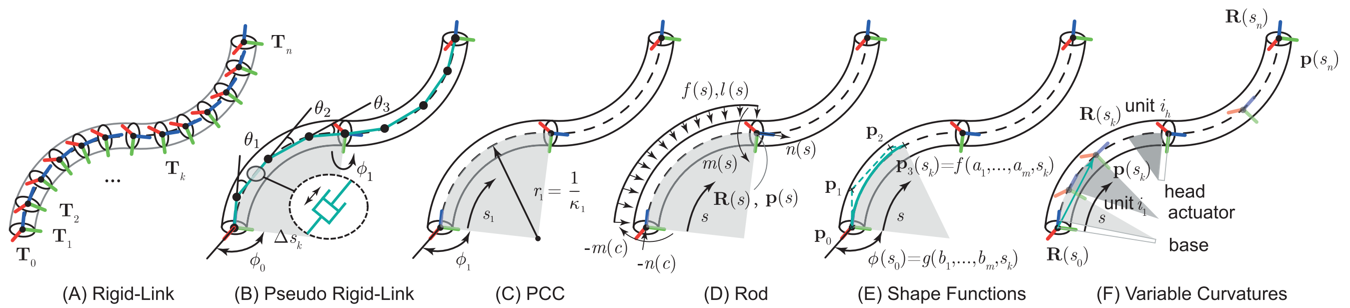

FIG. 3 Schematic of various kinematic frameworks used to describe the manipulator's geometry of rigid-link and soft continuum robots. The continuum robot with physical rigid-link can be represented by (A) Hyperredundant rigid-link structure with each physical joint represented by homogeneous transformation matrices; (B) Pseudo-rigid-link model to approximate a continuum body with a number of virtual links and rotational joints. Sometimes, passive prismatic joints are used. (C) Piecewise constant curvature (PCC) model is often used for rigid-link and soft continuum robots. It simplifies robot geometry by using constant curvature arcs. (D) Rod models, such as Cosserat rod and beam theory, are often used to represent robots. (E) Shape functions, such as the Bézier Curve, can be used to approximate the robot configuration in space. (F) Variable curvatures that consider the prototypical fact can sometimes better fit the robot's shape.

This section categorizes flexible manipulators by continuum robots with rigid links (i.e., backbone or notched-tube structure) and soft continuum manipulators (see Fig. 2). Such categorization is based on the fact that the continuum robots with discrete joints share some common kinematic knowledge with serial-link robots, while the soft continuum robots sometimes exhibit more complicated kinematics considering the nature of materials and soft mechanics.

Thus far, several kinematic frameworks have been proposed and utilized in MIS flexible robots. One can use different geometrical or algebraic models to describe flexible robot kinematics. Fig. 3 sketches a couple of model-based kinematic frameworks for discrete-jointed and soft continuum robots. The following subsections will briefly introduce these kinematic frameworks in robot-independent mapping, where the robot-dependent actuator space is not primarily considered. Since there are extensive reviews in the literature, this part provides only a concise description without rewinding the detailed mathematics derivation. As a handbook, useful literature for corresponding models will be provided.

Discrete-jointed continuum manipulators

A discrete-jointed continuum robot is a type of flexible robot, usually characterized by multiple degrees of freedom (DOF) and a finite number of rigid joint-link serial structures. Some may define them as "Semisoft" continuum robots [30], or "Rigid segment" continuum robots [31]. Table 2 lists some typical discrete-jointed continuum manipulators based on different kinematic models for MIS for the below case studies and discussions.

TABLE 2 Sample discrete-jointed and multibackbone continuum manipulators for MIS.

Ref.	Features	Main materials	Actuation methods	Kinematic models	Medical applications	Dimensions
[32]	13 rigid links with spherical joints	Polyether ether ketone (PEEK)	Cable driven	Discrete rigid-link model, CC	Manipulator	20 mm OD, 4 mm ID, 140 mm length
[33]	Proximally constrained bending motion, rigid vertebras	–	Cable driven	Discrete rigid-link model, CC	Manipulator	7.5 mm OD, length about 65 mm
[34]	17 rigid links with spherical joints and a gripper	NiTi backbone	Cable driven	Discrete rigid-link model, D-H	Maxillary sinus surgery/manipulator	4 mm OD, 30 mm length
[35]	Multiple 1D rolling joints, variable stiffness	ABS rolling joints	Cable driven	Discrete rigid-link model	Manipulator	20 mm OD, 12 mm ID
[36]	Notched structure	Metal	Cable driven	Pseudo-rigid-link (curve), D-H	Osteonecrosis, bone drilling	6 mm OD, 35 mm length
[37]	Hybrid motion/force control multibackbone	NiTi	Cable driven	PCC	Manipulator, haptic, tissue stiffness mapping	5 mm OD, 17.5 mm length for each segment
[38]	Tension propagation model with tendon friction considered	Stainless steel	Cable driven	PCC	Manipulator, endoscope	3.4 mm OD, 120 mm length
[39]	Three-segment continuum robot with multiple working channels	PTFE	Tendon-driven (pushing/pulling)	PCC	Transurethral bladder tumor resection	5 mm OD, three 1.8 mm ID working channels, 18, 20, 15 mm length, respectively
[40]	Two-segment continuum robot with shape-sensing capability	–	Cable driven	PCC/shape function	Manipulator	–
[41]	A rigid segment between two continuum segments with notched structures	Metal	Tendon driven (pushing/pulling)	Cosserat rod	Manipulator	–
[42]	With extensible sections and path-following motion	NiTi, magnets	Cable driven	Cosserat rod	Manipulator	5 mm OD, 15–55 mm segment length
[43]	RCM motion with a commercial robot arm	NiTi tube with notches	McKibben muscles (pneumatic)	Cosserat rod	Manipulator	7 mm OD, 6 mm ID, 66 mm length
[44]	FBG sensing	NiTi tube with notches	Cable-driven	Jacobian-approximated curvatures	Manipulator	6 mm OD, 34 mm length
[45]	3D-printed spring-like flexible joints with presettable stiffness	Metal	Tendon driven (pushing/pulling)	PCC with FEM-based correction	Manipulator	5 mm OD, 1.2 mm ID, 43.15 mm length
[46]	3-DOF, master-slave control	Titanium alloy	Cable driven	Learning based	Transoral laryngeal surgery/manipulator	6 mm OD, dual 2.1 mm ID, 52.5 mm length
[47]	Disc vertebras	PTFE tube backbone	Tendon driven	Learning based	Manipulator	8 mm OD, 100 mm length

Rigid-link model

Although the medical continuum robots listed in Table 2 are primarily assembled using rigid components, they exhibit compliant and flexible behavior upon actuation and interaction. Similar to the conventional kinematics models for rigid-link robots, one can use a homogeneous transformation matrix to represent the position and orientation of each link in space as

$$\mathbf{T}_i = \begin{bmatrix} \mathbf{R}_i & \mathbf{p}_i \\ \mathbf{0}_{1\times 3} & 1 \end{bmatrix} \in SE(3)$$

where $\mathbf{T}_i$ represents the "pose" of the i-th link with respect to some global coordinates, $\mathbf{R}_i \in SO(3)$ denotes the rotation matrix, and $\mathbf{p}_i \in \mathbb{R}^3$ is the position vector of a point on the link. When considering a Cartesian frame attached to the i-th link moves along with it, one can use $\mathbf{T}_i^{i-1}$ to describe the transformation from the $(i-1)$-th link to the i-th link. If one describes the pose of the i-th link with respect to a reference frame of {0}, it can be denoted by taking the continued multiplication of the successive frame as

$$\mathbf{T}_i^0 = \prod_{k=1}^{i} \mathbf{T}_k^{k-1}(\mathbf{q}_k)$$

where $\mathbf{q}_k \in \mathbb{R}^m$ represents the actuator variables, with m being the number of actuators. Fig. 3A provides a schematic of how the traditional serial-link kinematics can be applied to the modeling of continuum robots. It is often used by flexible robots with discrete rigid-link structures where they can be geometrically modeled. For MIS-oriented continuum robots, various joint-link structures have been proposed, such as those with spherical joints [32,34], serial vertebras [33], and rolling joints [35]. In particular, Piltan et al. [34] model a 4-DOF continuum robot composed of 17 discrete rigid links by using the Denavit-Hartenberg (D-H) convention [48]. However, hyperredundancy complicates the kinematics. With some proper assumptions on the robot geometry, the model can be simplified.

PCC

In fact, many experiments suggest that the continuum manipulators deform their shape continuously along the axial direction—which is mathematically equivalent to a rigid-link robot with infinitesimally tiny links and an infinite number of joints [24]. Therefore, early continuum robotics researchers established a simplified kinematic representation to describe the robots by using multiple serially connected circular arcs with constant curvatures, while each arc can be expressed by a finite set of parameters. This is usually referred to as a piecewise-constant curvature (PCC) model. It is termed based on the assumption that the curvature in each segment is constant over its longitudinal length upon bending. In PCC model, the forward kinematics can be written as

$$\mathbf{T}_i^0 = \prod_{k=1}^{i} \mathbf{T}_{cc,k}^{k-1}(\mathbf{\Psi}_k)$$

where $\mathbf{T}_{cc,k}^{k-1}(\mathbf{\Psi}_k)$ represents the local transformation (i.e., the i-th segment's) matrix with respect to its previous segment, and $\mathbf{\Psi}_k$ denotes the configuration variables in a vector form defining the geometry ("arc parameters") of the local curvature as

$$\mathbf{\Psi}_k(\mathbf{q}) = [\kappa_k \;\; \psi_k \;\; l_k]^\top$$

where κ_k, ψ_k, l_k represent the local curvature, angle of bending plane, and arc length, respectively (see Fig. 3C). The configuration of the local link is also a function of the actuator variables [15].

The arc geometry can also be represented by Frenet-Serret formulas (for example, in Ref. [49]) that parameterize a curve in terms of arc length s by defining a local coordinate frame, which moves along the curve in terms of a unit vector tangent to the curve $\boldsymbol{t}(s)$, a unit vector $\boldsymbol{n}(s)$, and a unit binormal vector $\boldsymbol{b}(s) = \boldsymbol{t}(s) \times \boldsymbol{n}(s)$, such that a coordinate along the arc can be obtained by taking the integration of the tangent curve as $\mathbf{p}(s) = \int_0^s \boldsymbol{t}(s)\mathrm{d}s$. Similar results can be obtained by using the exponential coordinates based on the Lie group theory [39,50,51] that decompose the homogeneous transformation of a constant curvature arc into rotation transformation and in-plane transformation. Note that those different representations are only diverse in mathematical forms but lead to the same CC assumptions. With many other variants and modified forms, the board-PCC model plays an essential role in soft and continuum robot kinematics modeling.

Cosserat rod

Modeling continuum robots using the Cosserat rod theory was first introduced by Trivedi et al. [52]. The method involves equilibrium relationships relating the internal and external forces and moments along the elastic robot backbone or robot body. As shown in Fig. 3D, the local rotation matrix and position vector along with the arc length with respect to a reference frame can be derived based on the differential kinematic relationship as

$$\frac{\mathrm{d}\mathbf{R}(s)}{\mathrm{d}s} = \mathbf{R}(s) \times u(s)$$

$$\frac{\mathrm{d}\mathbf{p}(s)}{\mathrm{d}s} = \mathbf{R}(s) \cdot v(s)$$

where $u(s) \in \mathbb{R}^3$ and $v(s) \in \mathbb{R}^3$ are the curvature vector containing angular rates of change about the rotation matrix and the linear velocity of the position vector, respectively. Considering the static equilibrium, the rod model consists of nonlinear ordinary differential equations (ODEs) for the internal force and moment vectors as [9]

$$\frac{\mathrm{d}n(s)}{\mathrm{d}s} + f(s) = 0$$
$$\frac{\mathrm{d}m(s)}{\mathrm{d}s} + \frac{\mathrm{d}\mathbf{p}(s)}{\mathrm{d}s} \times n(s) + l(s) = 0$$

where $n(s)$, $m(s)$, $f(s)$, and $l(s)$ are the vectors of internal force and moment, and vectors of external distributed force and moment, respectively. These equilibrium equations are generally coupled to the differential kinematic relationships through some material constitutive laws based on the material properties and mechanics. As it can satisfactorily describe the nonlinear strain-stress relationship, the method applies to many walks of the continuum and soft robots that obey elastic deformations upon actuation. In discrete-jointed continuum robots, the rod method is often used in modeling the elastic primary backbone that represents the continuum robot's curve. Recent examples that model medical discrete-jointed continuum robots using rod theory can be seen in Ref. [41, 42, 53].

Shape functions

Shape functions, usually in the form of curve parameters, can be used to approximate the continuum robot geometry and model the kinematics. One can describe the robot curve using linear combinations of mode shape functions as [29]

$$c(s) = \sum_{r=1}^{n} b_r \mathrm{M}_r(s)$$

where b_r denotes the r-th coefficient and M_r is the r-th shape functions. By principle, two curve parameters, namely, the curvature $\kappa(s)$ and angle of bending plane $\psi(s)$, are necessary to fully represent an in-plane bending. It is useful in the venue of continuum robotic sensing, where the general sensing techniques provide discrete instead of continuous data. One can employ the shape functions to estimate the geometry of continuum robots in space. For example, in Ref. [40], quadratic Bézier curves are used to reconstruct the wire-driven flexible robots with multiple bending segments by reading the discrete joint position and direction. In Ref. [54], piecewise cubic Bézier curves are employed to model a discrete-jointed continuum robot.

Jacobian approximation

Model-free approaches are also available to approximate the prototype-dependent kinematics of discrete-jointed continuum robots. In general, the velocity of a robot manipulator can be described by an input-output system of $\dot{\mathbf{x}} = \dot{f}(\mathbf{q})$ where the linear velocity of the end-effector $\dot{\mathbf{x}}$ is a first derivative function of the actuator inputs $\mathbf{q}$. The continuous function can be linearly approximated in an instantaneous status such that $\dot{\mathbf{x}} \approx \mathbf{J}\dot{\mathbf{q}}$, where $\mathbf{J}$ denotes the Jacobian matrix calculated by taking the partial derivatives of the $f(\mathbf{q})$. The Jacobian matrix that maps the actuator inputs and robot end-effector motion output can be empirically estimated—since the output can be physically measured using various methods, such as vision [55], FBGs [44], etc. However, when the system is redundant (i.e., there are multiple possible solutions given the same output), the method could be ineffective unless with more measurable outputs or higher dimensional output for the control. Even though the approximation is robot dependent, it provides a rapid numerical solution of the kinematics of a tangible continuum robot system.

Finite element

The variety of notched and hinge structures of continuum robots diversifies their kinematics. Finite element methods (FEM) are typically used to model the continuum robots in the venues where the robot morphology, internal/external force, and actuation are required to be included. FEM-enhanced kinematics could provide the correction terms subject to the new continuum robot design [45], design comparison and optimization [56], etc. Since there are quite a lot of rigid components in discrete-jointed continuum robots, the computational cost of FEM could be less expensive than that for soft-bodied robots.

Learning

It can be challenging to precisely model the continuum robots' kinematics due to the nonlinear factors such as friction and backlash in actuation, assembly error, robot gravity, payload, etc. Machine learning-based methods were long proposed to cope with the limitations of model-based kinematics, especially with the recent advancement of computational hardware and intelligent algorithms. Similar to the Jacobian approximation, machine learning-based methods are widely used in continuum robot kinematics by mapping the relationship between the input and output of the system. Nonlinear factors can be included in the learning, such as external payload [47], disturbances [57], master-side motion [46], etc. However, tedious data collection and offline training would become inevitable. Especially, reinforcement learning requires extensive interactions with the environment, which may cause damage to some types of continuum robots [58].

Here, we summarize the abovementioned kinematic models for discrete-jointed continuum robots in terms of robot dependency and model continuity using Fig. 4. Robot dependency shows the extent of the model's generality and rapid implementation among prototypes, while model continuity indicates the compliance of the robot description in different scenes. Given the same type of robots with known parameters, explicit mathematical methods often depend less on the prototypes from one to another. Robot kinematics can be rapidly implemented for control by adapting the parameters. On the contrary, the Jacobian approximation, FEM, and learning-based kinematics are more robot dependent, meaning that possible prototype differences cannot be easily identified by parameterization but by a re-run on either the simulation or real-world system—especially the learning-based kinematics modeling, which usually involves tedious data collection and offline training. This is a trade-off as the "model-less" methods often out weighted the "model-based" methods in terms of kinematics and statics accuracy. For medical applications, the major efforts on modeling have addressed the forward kinematics and static deflection, while the control has generally been solved from a quasistatic inverse kinematics perspective using traditional robotics knowledge like analytical and numerical (optimization, heuristics, and data-driven) methods.

Soft continuum manipulators

Soft continuum manipulators are primarily made from soft materials with low Young's modulus [59] comparable to human tissues. The soft nature guarantees interaction safety even in the worst-case scenarios where the robot-environment collision occurs; therefore, soft manipulators are becoming promising choices for developing RMIS tools [14]. Soft continuum manipulators demonstrate weak physical joint-link structures, higher deformability, and lower Poisson's ratio, making the modeling approaches not necessarily consistent with that of the discrete-linked continuum robots. The nonlinear nature of most soft materials—usually excluded from modeling rigid-bodied robots—will contribute to one of the significant factors that differentiate the kinematics of soft robots. With that being said, most of the kinematics models for discrete-linked continuum robots, except for the rigid-link model, are generally applicable to the soft manipulators by posing some assumptions. Table 3 lists some typical discrete-jointed continuum manipulators based on different kinematic models for MIS for the below case studies and discussions.

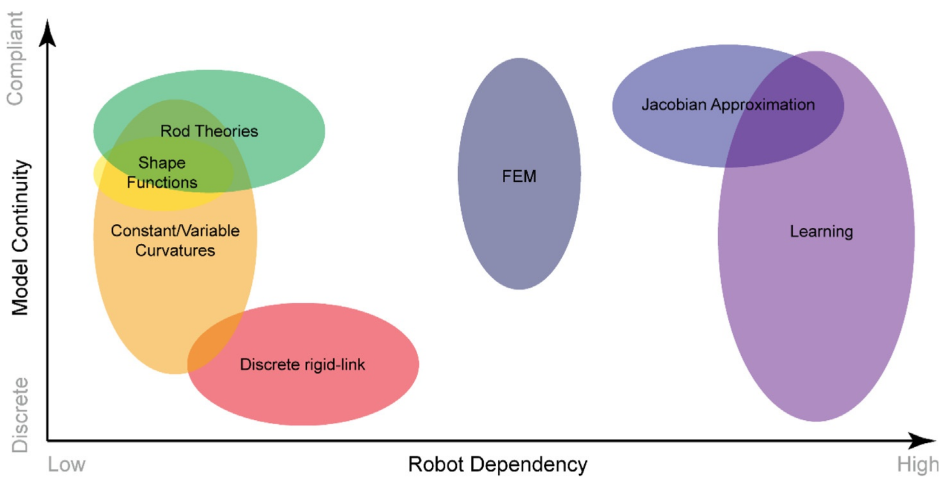

FIG. 4 The kinematic models for discrete-jointed continuum robots can be sketched out in terms of robot dependency and model continuity.

TABLE 3 Sample soft continuum manipulators for MIS.

Ref.	Features	Main materials	Actuation methods	Kinematic models	Medical applications	Dimensions
[60]	Single segment with four magnetic rings	Elastomer (PEBAX)	Magnetically actuated	PRB	Surgical catheter	2 mm OD, 1.2 mm ID, 52 mm length
[61]	Two segments, capable of elongation motion and variable stiffness. Cadaver study	Ecoflex 00-50	Fluidic driven	PCC	Manipulator	14.5 mm OD, 50 mm length
[62]	Two segments, visual-enhanced, configuration constraints	Agilus30 polymer	Cable driven	PCC	Blood suction tube	9 mm OD, 3.6 mm ID, 50 mm length per segment
[63]	Two segments, null space motion	Agilus30 polymer	Cable driven	PCC (variant)	Manipulator	9 mm OD, 3.6 mm ID, 50 mm length per segment
[64]	Single segment, capable of elongation and variable stiffness	Silicone rubber	Pneumatic driven	CC	Manipulator	25 mm OD, 13 mm ID, 50 mm length
[65]	Single segment with three channels for medical instruments	Silicone rubber	Cable driven	CC	Manipulator	10 mm OD, 45 mm length
[66]	Single segment, single actuation, variable stiffness	Ecoflex 00-50	Tendon and pneumatic	Cosserat rod	Manipulator	15 mm OD, 3 mm ID, 75 mm length
[67]	Two-segment, variable stiffness	Elastosil M4601 A/B	Cable driven	Cosserat rod	Manipulator	20 mm OD, 1.5 mm ID, 160 mm length
[68]	Single-segment, interactive navigation	Ecoflex 00-50	Fluidic driven	FEM-based Jacobian estimation	Manipulator	20 mm OD
[69]	Two segments, visual servoing with planar motion	PDMS	Cable driven	Visual servoing-based Jacobian estimation	Manipulator	9 mm OD, 50 mm length per segment
[70]	Single segment	Agilus30 polymer	Fluidic driven	Learning/FEM	MRI-guided transoral laser microsurgery	9.2 mm OD, 1.6 mm ID
[71]	Single segment with vision-based online learning	Ecoflex 00-50	Fluidic driven	Learning/FEM	Manipulator, endoscope	13 mm OD, 93 mm length
[72]	Two segments, sim-to-real visual servoing	Agilus30 polymer	Cable-driven	Learning/FEM (SOFA)	Manipulator, endoscope	6 mm OD, 50 mm length per segment
[73]	Single segment with locomotion	Ecoflex 00-30	Pneumatic driven	Empirical	Manipulator	25 mm OD, 15 mm ID
[74]	Single segment	PDMS	Pneumatic driven	Euler-Bernoulli Beam	Micromanipulator	1 mm OD
[75,76]	Single-segment, extrinsic tip controlled, extremely small	TPU, NdFeB (30% by volume)	Magnetically actuated	Euler-Bernoulli Beam	Surgical catheter	0.5–0.6 mm OD

Pseudo-rigid-body

As soft manipulators are, in most cases, composed of multiple pieces of soft elastic segments that deform in continuous configurations, the rigid-link model would be inapplicable. However, one can assume the continuum segment as a pseudo-rigid-body (PRB, or pseudo-rigid-link) structure, a widely used modeling assumption in compliant mechanics. Although the PRB models generally consist of a finite number of serially connected pseudo-links, their modeling conventions can vary depending on the accuracy requirement. There are several PRB models reported in the literature. For example, in Ref. [60], the authors model a single soft segment using a 6-DOF PRB model with four pseudo-rigid links connected by three rotational joints. The highly customizable PRB links fit the soft magnetic catheters with heterogeneously distributed magnets. In Ref. [77], a soft segment is simplified as two pseudo-links with passive variable length connected by a rotational joint. Several PRB conventions for soft robots, such as RPR, RPPR, and RPRPR, are raised and discussed in Ref. [78]. The method is also applicable to describe the elastic backbones of the discrete-jointed continuum robots.

PCC

The PCC modeling method is also applicable to the soft-bodied continuum robots following the same assumptions [61,62,65], usually with virtual backbones to represent the soft body's geometry. However, the original PCC convention does not primarily consider the soft materials property, external load, or physical contact with the environment. Common phenomena like elongation, shrinkage, and nonlinear inflation that occur on soft manipulators would be neglected by the PCC assumptions unless with model modification. There are several modified PCC models that enhance the model adaptiveness for soft manipulators. The use of different methods for PCC modification has been reported, such as incorporating FEM [79,80] or augmented PRB model [81], considering the soft body mechanics [63], mode shape function-based variable curvature [82], etc. Therefore, there is still plenty of room to modify the CC convention for different soft manipulators based on the robot designs and prototypes.

Cosserat rod

Cosserat rod theory frameworks are one of the ideal choices for soft-bodied robot modeling, as they describe a material-dependent homogeneous transformation frame to express the "backbone" as a function of the arc length along the robot. The rod theory frameworks are friendly to the description and investigation of variable stiffness soft robots for medical applications [66,67] related to the material's nonlinearity, external payload, and actuation mechanics. Variant rod methods have also been developed. For instance, a compromise method called piecewise constant strain (PCS) was proposed by Renda et al. [83], which discretizes the Cosserat rod method and assumes piecewise constant deformation along the soft body (inspired by the PCC) to achieve simplification, benefiting the model adaptability.

Others

Other kinematics modeling methods for soft manipulators are similar to that of the discrete-jointed continuum robots, including FEM, mechanics beam, Jacobian estimation, machine learning, empiricism, etc. Among them, FEM and mechanics methods can be established independently from prototypes, while the others are robot-dependent unless with some fusions. For example, the finite element analysis (FEA) can partially become a source for the Jacobian estimation [68] or machine learning [70]. In Ref. [71], the FEA-based model of a single-bending soft robot is used to initialize the online learning supported by the ground truth measurement from the prototype—which greatly reduces the computational complexity and makes the Jacobian initialization easier. For soft robots with simple nonlinear bending motion, one can empirically map the kinematic relationship [73]. Millimeter-grade soft robotic catheters are usually magnetically tip-driven to navigate through complex environments like blood vessels and bronchia. These types of soft robots are partially bent at their tip to "switch" direction by the amplitude of the electromagnetic field and directly dragged by the locatable magnetic source. The intrinsic actuation allows symmetrical force distribution. Hence, the catheters can be ideally modeled as short cantilever beams [75,76].

In this section, we would like to summarize the soft robots' kinematics by their conveniences and competency in describing the nonlinearity of the robot's motion. Fig. 5 demonstrates an overview of the summary. Geometry-based methods like PCC and PRBs are relatively limited in expressing the robot's nonlinear behavior but benefit rapid kinematics modeling with available parameters. Their nonlinearity can be further enhanced by fusing other methods. Rod and beam theories are capable of illustrating the soft robot's physical behaviors related to internal and external forces. Model-free methods that employ fine meshes or experimental data generally neglect geometry complexity and nonlinearity. Therefore, they can derive the kinematics of some highly customized soft manipulators.

Kinematics-based applications for MIS flexible robots

There is a growing trend that flexible manipulators are being adopted as the end-effectors of RMIS because of the inherent interaction safety. For flexible robots, kinematics is fundamental for many MIS applications that require precise control. When there is a new MIS flexible robotic tool being designed, a thorough study of kinematics would provide a clear prediction of how the robot behaves, how we can have better control, and even suggest how we can take advantage of the compliant structures. In this part, we introduce several kinematics-based RMIS applications for flexible robots by case study.

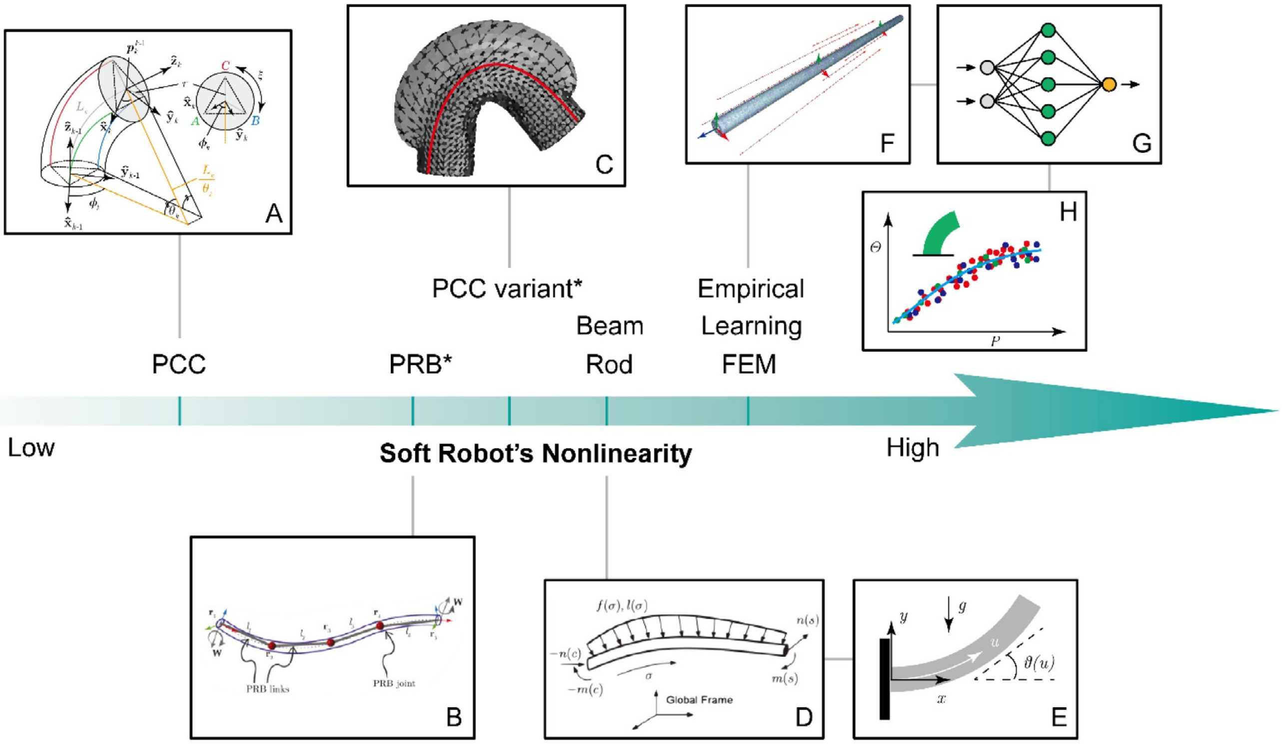

FIG. 5 Different kinematics modeling methods for soft robots in terms of the conveniences in expressing nonlinearity: (A) PCC is often used in soft robotic kinematics; (B) PRBs can describe complicated soft robots' motion with sufficient control point; (C) PCC can be further improved by incorporating other modeling factors; (D) Cosserat rod theory includes forces in the modeling; (E) Euler-Bernoulli beam theory are often used in describing soft robots with simple bending with some ideal assumptions; (F) FEM, (G) machine learning, and (H) empirical methods are competent of describe highly nonlinear soft robot behavior despite of the model complexity.

Workspace optimization

The workspace is typically defined as a set of endpoints that can be approached by the end-effector of the manipulators. Generally, the robot's end-effector is repositioned by bending the continuum structure in a confined environment without excessively pivoting around the incision/trocar. As shown in Fig. 6A, this could significantly reduce the motion of the robot's footprint (operational space) and improve the end-effector's workspace, which is helpful to the maturation of specific RMIS and improvement of interaction safety. While using flexible robots with simple bending structures and RCM (remote-center-of-motion), mechanism can improve the end-effector's workspace, employing multisegment flexible tools can even reduce the operation space that prevents the tools from pivoting around the incision.

In this regard, model-based kinematics can be employed to investigate and optimize the end-effector workspace prior to robot fabrication. It allows the researchers to tailor design flexible robotic tools for different surgical venues. For example, Li et al. [84] explicitly analyzed the workspace of a discrete-jointed cable-driven continuum manipulator with different longitudinal constraints based on the PCC model. By partially constraining the proximal segment from bending, single-segment robots could attain a wider workspace without adding extra DOF to the system. In Ref. [85], the authors optimized the multisegment continuum robot design according to the reachable workspace and desired functional volume with the help of PCC modeling. In addition to the kinematics, static analysis can be incorporated into the PCC in estimating the end-effector's workspace [86], such that different forces would be included in the modeling. For soft material-based robots, FEM modeling [71,87] could provide an intuitive sensation of workspace that allows one to optimize the parameters in not only robot geometry but also physical properties like morphology and the use of materials. In Ref. [88], Cosserat rod models were employed to analyze a hybrid rigid-flexible soft robot with the consideration of material constitutive law. Other kinematic models are also often used in estimating the soft robot's workspace that fits biomedical applications. In Ref. [89], a beam model was used to compute the soft robotic end-effector's spatial position and further bioprinting control in MIS. Supported by the field data, Lin et al. [90] reported a flexible magnetic-driven continuum robot with enlarged effectiveness in constrained conditions for retrograde intrarenal surgery. Fig. 6B summarizes the general workflow of how workspace optimization works with kinematic analysis during the design stage of a standalone flexible robotic tool for MIS.

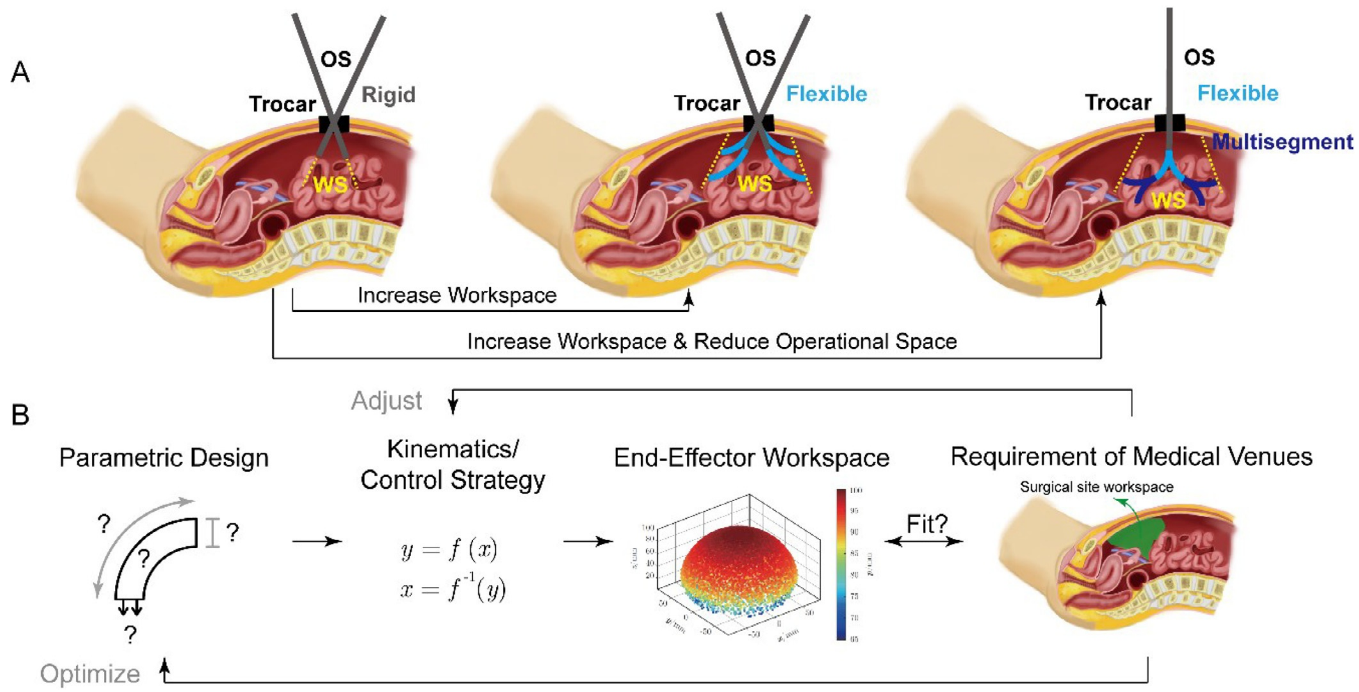

FIG. 6 (A) Compared to rigid RMIS tools, using flexible RMIS tools can increase the end-effector's workspace and reduce the footprint's operational space. (B) General workflow of workspace optimization for RMIS flexible robotic tools.

Motion constraints

Instead of operating in free space, MIS flexible robots are often expected to work in confined, obstructed environments that could possibly constrain the robot's motion. In this regard, the kinematics of flexible robots can be modified and further investigated to fit the MIS scenes. Several kinematics-based flexible robot motions considered constraints have been published in the past decade. For example, Bajo and Simaan [91] derived the constrained differential kinematics based on the PCC model to detect and localize the contacts along a surgical multisegment continuum robot. The methods were further applied to the transurethral bladder resection task [92]. In another work from them [37], they presented a framework that compromises the PCC-based robot motion and force controller to estimate the stiffness and shape of the external objects and environment on a multibackbone continuum robot for MIS. In Ref. [62], a configuration constraint was assigned to a two-segment PCC-based soft robot to regulate the end-effector's orientation with respect to the task surface for effective blood suction. Follow-the-leader motion, which is desirable for many MIS applications, was developed for tendon-driven continuum robots based on the Cosserat rod model [93]. Sensor-based online Jacobian estimation methods were introduced to control continuum manipulators to work in constrained environments [55] and even perform soft object manipulation [94,95].

Except for making use of the kinematics of standalone miniature multisegment robots, one can associate the macro-robot arm and attain extra degrees of freedom that compensate the microrobots with simple 2-DOF bending motion (i.e., single-segment continuum robots). This is often seen when the macro-micro MIS robots are coupled as one piece. The task space operations can be performed through the RCM constraints enabled by redundant kinematics—which raises worthy optimization problems in multiple solutions for the joint space control. For example, a spherical linkage RCM mechanism with a single-segment discrete-jointed continuum robot was proposed by Qi et al. [96]. The end-effector's motion of the PCC-modeled robot was mechanically constrained, and the tip motion could be kinematically modeled by extending the base frame. In Ref. [97], the authors attached a cable-driven continuum robot with a single bending segment onto a commercial robot arm (UR5) to obtain RCM motion. The RCM constraints formulated a QP problem with multiple cost functions to realize multi-DOF kinematic control. Similar works can be found in Ref. [98], which proposes a convex optimization method to control a micro-macro robotic motion with alternating direction method of multipliers (ADMM) and damped least square (DLM) algorithms. Recently, Alambeigi et al. [99] report using such a robotic system for orthopedic MIS, showing the competency and performance of employing motion constraint strategy on flexible robots for RMIS applications.

Conclusions

This chapter provides a concise overview of how kinematics concepts are utilized in RMIS with flexible robotic manipulators. We limit our focus to the recent decade and subjects of discrete-jointed and soft continuum robots for potential RMIS applications. Through state-of-the-art case studies, we cover kinematic modeling methods with multidimensional comparisons and their practical applications. Our discussion is confined to the literature on MIS flexible robots, which provides realistic and reproducible references on how flexible robots are designed, considered, and adopted in medical applications. In terms of applications, we address workspace optimization and motion constraints, which can be resolved by investigating robot kinematics. Overall, this chapter serves as a valuable resource for researchers, medical robot designers, and developers by providing a comprehensive overview of the recent advances in the kinematic modeling of flexible robotic manipulators in RMIS and their practical applications.

Future scenario

The authors contend that there is still considerable potential for the development and refinement of flexible robotic kinematics. As flexible robots become increasingly softer, lighter, and smaller, they are becoming more versatile and multifunctional in terms of robotic motion and control. This presents a significant challenge to the efficacy of kinematics modeling for RMIS applications. Moreover, comprehensive RMIS scenarios still pose significant challenges to the kinematics and statics of continuum robots. Meanwhile, new types of flexible robots are evolving, which may require model revisions or even new models. However, the authors remain optimistic that ongoing research efforts will lead to the continued advancement and evolution of flexible robotic manipulators in RMIS, ultimately improving patient outcomes and medical procedures.

Key points

- Kinematic concepts in MIS flexible robotic manipulators through case studies of the recent decade (2012–22) are described.
- Two types of MIS flexible robotic manipulators have been extensively investigated in the field, namely, the flexible manipulators and the soft continuum manipulators. Both of them share similar kinematic modeling concepts, but the latter demonstrates more room for exploration.
- The kinematics-based applications for MIS flexible robots are challenging to fit the intended clinical scenarios. More medical critiques can be considered in the robot design and kinematics.

Acknowledgment

This work was supported by Hong Kong Research Grants Council (RGC) Collaborative Research Fund (C4026-21G), Research Grants Council (RGC)—Research Impact Fund (RIF R4020-22), General Research Fund (GRF 14211420), Research Grants Council (RGC)—NSFC/RGC Joint Research Scheme N_CUHK420/22, Shenzhen-Hong Kong-Macau Technology Research Programme (Type C) STIC Grant SGDX20210823103535014 (202108233000303) the key project 2021B1515120035 (B.02.21.00101) of the Regional Joint Fund Project of the Basic and Applied Research Fund of Guangdong Province, Hong Kong Research Grants Council (RGC) Collaborative Research Fund (CRF C4063-18G and C4026-21G), General Research Funds (GRF 14216022, GRF 14203323), CUHK IdeaBooster Fund Award (IDBF23ENG06), and CUHK Faculty Direct Grant (4055213).

References

[1] Sachs J, Andersson LAA, Araújo J, Curescu C, Lundsjö J, Rune G, Steinbach E, Wikström G. Adaptive 5G low-latency communication for tactile internet services. Proc IEEE 2019;107:325–49.

[2] Taylor RH, Menciassi A, Fichtinger G, Fiorini P, Dario P. Medical robotics and computer-integrated surgery. In: Springer handbook of robotics. Springer; 2016. p. 1657–84.

[3] de Smet MD, Naus GJL, Faridpooya K, Mura M. Robotic-assisted surgery in ophthalmology. Curr Opin Ophthalmol 2018;29:248–53.

[4] Sharifi M, Salarieh H, Behzadipour S, Tavakoli M. Beating-heart robotic surgery using bilateral impedance control: theory and experiments. Biomed Signal Process Control 2018;45:256–66.

[5] Li S, Ai Q, Liang H, Liu H, Yang C, Deng H, Zhong Y, Zhang J, He J. Nonintubated robotic-assisted thoracic surgery for tracheal/airway resection and reconstruction: technique description and preliminary results. Ann Surg 2022;275, e534.

[6] Kinross JM, Mason SE, Mylonas G, Darzi A. Next-generation robotics in gastrointestinal surgery. Nat Rev Gastroenterol Hepatol 2020;17:430–40.

[7] Yip HM, Wang Z, Navarro-Alarcon D, Li P, Cheung TH, Greiffenhagen C, Liu Y-h. A collaborative robotic uterine positioning system for laparoscopic hysterectomy: design and experiments. Int J Med Robot Comput Assist Surg 2020;16, e2103.
[8] Min Z, Wang J, Pan J, Meng MQ-H. Generalized 3-D point set registration with hybrid mixture models for computer-assisted orthopedic surgery: from isotropic to anisotropic positional error. IEEE Trans Autom Sci Eng 2020;18:1679–91.
[9] Burgner-Kahrs J, Rucker DC, Choset H. Continuum robots for medical applications: a survey. IEEE Trans Robot 2015;31:1261–80.
[10] Kwok K-W, Wurdemann H, Arezzo A, Menciassi A, Althoefer K. Soft robot-assisted minimally invasive surgery and interventions: advances and outlook. Proc IEEE 2022;110:871–92.
[11] Dobbs RW, Halgrimson WR, Madueke I, Vigneswaran HT, Wilson JO, Crivellaro S. Single-port robot-assisted laparoscopic radical prostatectomy: initial experience and technique with the da Vinci® SP platform. BJU Int 2019;124:1022–7.
[12] Chen Y, Zhang C, Wu Z, Zhao J, Yang B, Huang J, et al. The SHURUI system: a modular continuum surgical robotic platform for multiport, hybrid-port, and single-port procedures. IEEE/ASME Trans Mechatron 2022;27(5):3186–97. https://doi.org/10.1109/TMECH.2021.3110883.
[13] Lang S, Mattheis S, Hasskamp P, Lawson G, Güldner C, Mandapathil M, Schuler P, Hoffmann T, Scheithauer M, Remacle M. A European multicenter study evaluating the flex robotic system in transoral robotic surgery. Laryngoscope 2017;127:391–5.
[14] Runciman M, Darzi A, Mylonas GP. Soft robotics in minimally invasive surgery. Soft Robot 2019;6:423–43.
[15] Webster III RJ, Jones BA. Design and kinematic modeling of constant curvature continuum robots: a review. Int J Robot Res 2010;29:1661–83.
[16] Zhong Y, Hu L, Xu Y. Recent advances in design and actuation of continuum robots for medical applications. Actuators 2020;9(4):142. https://doi.org/10.3390/act9040142.
[17] Thuruthel TG, Shih B, Laschi C, Tolley MT. Soft robot perception using embedded soft sensors and recurrent neural networks. Sci Robot 2019;4, eaav1488.
[18] Zhang Y, Lu M. A review of recent advancements in soft and flexible robots for medical applications. Int J Med Robot Comput Assist Surg 2020;16, e2096.
[19] da Veiga T, Chandler JH, Lloyd P, Pittiglio G, Wilkinson NJ, Hoshiar AK, Harris RA, Valdastri P. Challenges of continuum robots in clinical context: a review. Prog Biomed Eng 2020;2:032003.
[20] Shi C, Luo X, Qi P, Li T, Song S, Najdovski Z, Fukuda T, Ren H. Shape sensing techniques for continuum robots in minimally invasive surgery: a survey. IEEE Trans Biomed Eng 2016;64:1665–78.
[21] Cao Y, Shi Y, Hong W, Dai P, Sun X, Yu H, Xie L. Continuum robots for endoscopic sinus surgery: recent advances, challenges, and prospects. Int J Med Robot Comput Assist Surg 2022; e2471.
[22] Gifari MW, Naghibi H, Stramigioli S, Abayazid M. A review on recent advances in soft surgical robots for endoscopic applications. Int J Med Robot Comput Assist Surg 2019;15, e2010.
[23] Dupont PE, Nelson BJ, Goldfarb M, Hannaford B, Menciassi A, O'Malley MK, Simaan N, Valdastri P, Yang G-Z. A decade retrospective of medical robotics research from 2010 to 2020. Sci Robot 2021;6, eabi8017.
[24] Dupont PE, Simaan N, Choset H, Rucker C. Continuum robots for medical interventions. Proc IEEE 2022;110:847–70.
[25] George Thuruthel T, Ansari Y, Falotico E, Laschi C. Control strategies for soft robotic manipulators: a survey. Soft Robot 2018;5:149–63.
[26] Li Z, Wu L, Ren H, Yu H. Kinematic comparison of surgical tendon-driven manipulators and concentric tube manipulators. Mech Mach Theory 2017;107:148–65.
[27] Armanini C, Messer C, Mathew AT, Boyer F, Duriez C, Renda F. Soft robots modeling: A structured overview. arXiv preprint arXiv:2112.03645; 2021.
[28] Barrientos-Diez J, Dong X, Axinte D, Kell J. Real-time kinematics of continuum robots: modelling and validation. Robot Comput Integr Manuf 2021;67:102019.
[29] Rao P, Peyron Q, Lilge S, Burgner-Kahrs J. How to model tendon-driven continuum robots and benchmark modelling performance. Front Rob AI 2021;7:630245.
[30] Li S, Hao G. Current trends and prospects in compliant continuum robots: a survey. Actuators 2021;10(7):145. https://doi.org/10.3390/act10070145.
[31] Tan N, Gu X, Ren H. Design, characterization and applications of a novel soft actuator driven by flexible shafts. Mech Mach Theory 2018;122:197–218.
[32] Ji D, Kang TH, Shim S, Lee S, Hong J. Wire-driven flexible manipulator with constrained spherical joints for minimally invasive surgery. Int J Comput Assist Radiol Surg 2019;14:1365–77.
[33] Li Z, Feiling J, Ren H, Yu H. A novel tele-operated flexible robot targeted for minimally invasive robotic surgery. Engineering 2015;1:073–8.
[34] Piltan F, Kim C-H, Kim J-M. Adaptive fuzzy-based fault-tolerant control of a continuum robotic system for maxillary sinus surgery. Appl Sci 2019;9:2490.
[35] Kim Y-J, Cheng S, Kim S, Iagnemma K. A stiffness-adjustable hyperredundant manipulator using a variable neutral-line mechanism for minimally invasive surgery. IEEE Trans Robot 2013;30:382–95.
[36] Alambeigi F, Wang Y, Sefati S, Gao C, Murphy RJ, Iordachita I, Taylor RH, Khanuja H, Armand M. A curved-drilling approach in core decompression of the femoral head osteonecrosis using a continuum manipulator. IEEE Robot Autom Lett 2017;2:1480–7.
[37] Bajo A, Simaan N. Hybrid motion/force control of multi-backbone continuum robots. Int J Robot Res 2016;35:422–34.
[38] Kato T, Okumura I, Song S-E, Golby AJ, Hata N. Tendon-driven continuum robot for endoscopic surgery: preclinical development and validation of a tension propagation model. IEEE/ASME Trans Mechatron 2014;20:2252–63.
[39] Sarli N, Del Giudice G, De S, Dietrich MS, Herrell SD, Simaan N. TURBot: a system for robot-assisted transurethral bladder tumor resection. IEEE/ASME Trans Mechatron 2019;24:1452–63.
[40] Song S, Li Z, Meng MQ-H, Yu H, Ren H. Real-time shape estimation for wire-driven flexible robots with multiple bending sections based on quadratic Bézier curves. IEEE Sensors J 2015;15:6326–34.
[41] Zhao B, Zeng L, Wu Z, Xu K. A continuum manipulator for continuously variable stiffness and its stiffness control formulation. Mech Mach Theory 2020;149:103746.
[42] Amanov E, Nguyen T-D, Burgner-Kahrs J. Tendon-driven continuum robots with extensible sections—a model-based evaluation of path-following motions. Int J Robot Res 2021;40:7–23.

[43] Smoljkic G, Borghesan G, Devreker A, Poorten EV, Rosa B, De Praetere H, De Schutter J, Reynaerts D, Sloten JV. Control of a hybrid robotic system for computer-assisted interventions in dynamic environments. Int J Comput Assist Radiol Surg 2016;11:1371–83.
[44] Sefati S, Murphy RJ, Alambeigi F, Pozin M, Iordachita I, Taylor RH, Armand M. FBG-based control of a continuum manipulator interacting with obstacles. In: 2018 IEEE/RSJ international conference on intelligent robots and systems (IROS); 2018.
[45] Feng F, Hong W, Xie L. Design of 3D-printed flexible joints with presettable stiffness for surgical robots. IEEE Access 2020;8:79573–85.
[46] Feng F, Zhou Y, Hong W, Li K, Xie L. Development and experiments of a continuum robotic system for transoral laryngeal surgery. Int J Comput Assist Radiol Surg 2022;17:497–505.
[47] Wang Z, Wang T, Zhao B, He Y, Hu Y, Li B, Zhang P, Meng MQ-H. Hybrid adaptive control strategy for continuum surgical robot under external load. IEEE Robot Autom Lett 2021;6:1407–14.
[48] Corke PI. A simple and systematic approach to assigning Denavit–Hartenberg parameters. IEEE Trans Robot 2007;23:590–4.
[49] Ros-Freixedes L, Gao A, Liu N, Shen M, Yang G-Z. Design optimization of a contact-aided continuum robot for endobronchial interventions based on anatomical constraints. Int J Comput Assist Radiol Surg 2019;14:1137–46.
[50] Murray RM, Li Z, Sastry SS. A mathematical introduction to robotic manipulation. CRC Press; 2017.
[51] Grazioso S, Gironimo GD, Siciliano B. From differential geometry of curves to helical kinematics of continuum robots using exponential mapping. In: International symposium on advances in robot kinematics; 2018.
[52] Trivedi D, Lotfi A, Rahn CD. Geometrically exact models for soft robotic manipulators. IEEE Trans Robot 2008;24:773–80.
[53] Mitros Z, Thamo B, Bergeles C, Da Cruz L, Dhaliwal K, Khadem M. Design and modelling of a continuum robot for distal lung sampling in mechanically ventilated patients in critical care. Front Rob AI 2021;8:611866.
[54] Guo H, Ju F, Chen B. Preliminary study on shape sensing for continuum robot affected by external load using piecewise fitting curves. In: 2019 IEEE international conference on robotics and biomimetics (ROBIO); 2019.
[55] Yip MC, Camarillo DB. Model-less feedback control of continuum manipulators in constrained environments. IEEE Trans Robot 2014;30:880–9.
[56] Tian J, Wang T, Fang X, Shi Z. Design, fabrication and modeling analysis of a spiral support structure with superelastic Ni-Ti shape memory alloy for continuum robot. Smart Mater Struct 2020;29:045007.
[57] Cui Z, Li J, Li W, Zhang X, Chiu PWY, Li Z. Fast convergent antinoise dual neural network controller with adaptive gain for flexible endoscope robots. IEEE Trans Neural Netw Learn Syst 2022.
[58] Tan N, Yu P, Zhong Z, Zhang Y. Data-driven control for continuum robots based on discrete zeroing neural networks. IEEE Trans Ind Inform 2022.
[59] Rus D, Tolley MT. Design, fabrication and control of soft robots. Nature 2015;521:467–75.
[60] Venkiteswaran VK, Sikorski J, Misra S. Shape and contact force estimation of continuum manipulators using pseudo rigid body models. Mech Mach Theory 2019;139:34–45.
[61] Abidi H, Gerboni G, Brancadoro M, Fras J, Diodato A, Cianchetti M, Wurdemann H, Althoefer K, Menciassi A. Highly dexterous 2-module soft robot for intra-organ navigation in minimally invasive surgery. Int J Med Robot Comput Assist Surg 2018;14, e1875.
[62] Lai J, Huang K, Lu B, Zhao Q, Chu HK. Verticalized-tip trajectory tracking of a 3D-printable soft continuum robot: enabling surgical blood suction automation. IEEE/ASME Trans Mechatron 2021;27:1545–56.
[63] Lai J, Lu B, Zhao Q, Chu HK. Constrained motion planning of a cable-driven soft robot with compressible curvature modeling. IEEE Robot Autom Lett 2022;7:4813–20.
[64] Ranzani T, Cianchetti M, Gerboni G, De Falco I, Menciassi A. A soft modular manipulator for minimally invasive surgery: design and characterization of a single module. IEEE Trans Robot 2016;32:187–200.
[65] Li R, Chen F, Yu W, Igarash T, Shu X, Xie L. A novel cable-driven soft robot for surgery. J Shanghai Jiaotong Univ (Sci) 2022;1–13.
[66] Roshanfar M, Sayadi A, Dargahi J, Hooshiar A. Stiffness adaptation of a hybrid soft surgical robot for improved safety in interventional surgery. In: 2022 44th annual international conference of the IEEE Engineering in Medicine & Biology Society (EMBC); 2022.
[67] Xiao Q, Musa M, Godage I, Su H, Chen Y. Kinematics and stiffness modeling of soft robot with a concentric backbone. J Mech Robot 2022;1–13.
[68] Lee K-H, Leong MCW, Chow MCK, Fu H-C, Luk W, Sze K-Y, Yeung C-K, Kwok K-W. FEM-based soft robotic control framework for intracavitary navigation. In: 2017 IEEE international conference on real-time computing and robotics (RCAR); 2017.
[69] Lai J, Huang K, Lu B, Chu HK. Toward vision-based adaptive configuring of a bidirectional two-segment soft continuum manipulator. In: 2020 IEEE/ASME international conference on advanced intelligent mechatronics (AIM); 2020.
[70] Fang G, Chow MCK, Ho JDL, He Z, Wang K, Ng TC, Tsoi JKH, Chan P-L, Chang H-C, Chan DT-M, et al. Soft robotic manipulator for intraoperative MRI-guided transoral laser microsurgery. Sci Robot 2021;6, eabg5575.
[71] Lee K-H, Fu DKC, Leong MCW, Chow M, Fu H-C, Althoefer K, Sze KY, Yeung C-K, Kwok K-W. Nonparametric online learning control for soft continuum robot: an enabling technique for effective endoscopic navigation. Soft Robot 2017;4:324–37.
[72] Lai J, Ren T-A, Yue W, Su S, Chan JYK, Ren H. Sim-to-real transfer of soft robotic navigation strategies that learns from the virtual eye-in-hand vision. IEEE Trans Ind Inform 2024;20:2365–77.
[73] Zhang B, Fan Y, Yang P, Cao T, Liao H. Worm-like soft robot for complicated tubular environments. Soft Robot 2019;6:399–413.
[74] Gorissen B, Vincentie W, Al-Bender F, Reynaerts D, De Volder M. Modeling and bonding-free fabrication of flexible fluidic microactuators with a bending motion. J Micromech Microeng 2013;23:045012.
[75] Wang L, Kim Y, Guo CF, Zhao X. Hard-magnetic elastica. J Mech Phys Solids 2020;142:104045.
[76] Kim Y, Parada GA, Liu S, Zhao X. Ferromagnetic soft continuum robots. Sci Robot 2019;4, eaax7329.
[77] Lai J, Huang K, Chu HK. A learning-based inverse kinematics solver for a multi-segment continuum robot in robot-independent mapping. In: 2019 IEEE international conference on robotics and biomimetics (ROBIO); 2019.
[78] Santina CD, Katzschmann RK, Bicchi A, Rus D. Model-based dynamic feedback control of a planar soft robot: trajectory tracking and interaction with the environment. Int J Robot Res 2020;39:490–513.
[79] Runge G, Wiese M, Günther L, Raatz A. A framework for the kinematic modeling of soft material robots combining finite element analysis and piecewise constant curvature kinematics. In: 2017 3rd international conference on control, automation and robotics (ICCAR); 2017.
[80] Caasenbrood B, Pogromsky A, Nijmeijer H. Control-oriented models for hyperelastic soft robots through differential geometry of curves. Soft Robot 2023;10(1):129–48.

[81] Katzschmann RK, Della Santina C, Toshimitsu Y, Bicchi A, Rus D. Dynamic motion control of multi-segment soft robots using piecewise constant curvature matched with an augmented rigid body model. In: 2019 2nd IEEE international conference on soft robotics (RoboSoft); 2019.

[82] Godage IS, Medrano-Cerda GA, Branson DT, Guglielmino E, Caldwell DG. Modal kinematics for multisection continuum arms. Bioinspir Biomim 2015;10:035002.

[83] Renda F, Cacucciolo V, Dias J, Seneviratne L. Discrete Cosserat approach for soft robot dynamics: a new piece-wise constant strain model with torsion and shears. In: 2016 IEEE/RSJ international conference on intelligent robots and systems (IROS); 2016.

[84] Li Z, Ren H, Chiu PWY, Du R, Yu H. A novel constrained wire-driven flexible mechanism and its kinematic analysis. Mech Mach Theory 2016;95:59–75.

[85] Xu K, Zhao J, Zheng X. Configuration comparison among kinematically optimized continuum manipulators for robotic surgeries through a single access port. Robotica 2015;33:2025–44.

[86] Yuan H, Li Z. Workspace analysis of cable-driven continuum manipulators based on static model. Robot Comput Integr Manuf 2018;49:240–52.

[87] Amehri W, Zheng G, Kruszewski A. Fem based workspace estimation for soft robots: a forward-backward interval analysis approach. In: 2020 3rd IEEE international conference on soft robotics (RoboSoft); 2020.

[88] Altuzarra O, Solanillas DM, Amezua E, Petuya V. Path analysis for hybrid rigid–flexible mechanisms. Mathematics 2021;9:1869.

[89] Zhou C, Yang Y, Wang J, Wu Q, Gu Z, Zhou Y, Liu X, Yang Y, Tang H, Ling Q, et al. Ferromagnetic soft catheter robots for minimally invasive bioprinting. Nat Commun 2021;12:1–12.

[90] Lin D, Wang J, Jiao N, Wang Z, Liu L. A flexible magnetically controlled continuum robot steering in the enlarged effective workspace with constraints for retrograde intrarenal surgery. Adv Intell Syst 2021;3:2000211.

[91] Bajo A, Simaan N. Kinematics-based detection and localization of contacts along multisegment continuum robots. IEEE Trans Robot 2011;28:291–302.

[92] Bajo A, Pickens RB, Herrell SD, Simaan N. Constrained motion control of multisegment continuum robots for transurethral bladder resection and surveillance. In: 2013 IEEE international conference on robotics and automation (ICRA); 2013.

[93] Neumann M, Burgner-Kahrs J. Considerations for follow-the-leader motion of extensible tendon-driven continuum robots. In: 2016 IEEE international conference on robotics and automation (ICRA); 2016.

[94] Mo H, Ouyang B, Xing L, Dong D, Liu Y, Sun D. Automated 3-D deformation of a soft object using a continuum robot. IEEE Trans Autom Sci Eng 2020;18:2076–86.

[95] Lai J, Lu B, Huang K, Chu HK. Gesture-based steering framework for redundant soft robots. IEEE/ASME Trans Mechatron 2024;1–13.

[96] Qi P, Zhang C, Li J, Li Z, Dai JS, Althoefer K. A compact continuum manipulator system with enhanced steering abilities for robot-assisted surgery. In: 2016 6th IEEE international conference on biomedical robotics and biomechatronics (BioRob); 2016.

[97] Zhang X, Li W, Chiu PWY, Li Z. A novel flexible robotic endoscope with constrained tendon-driven continuum mechanism. IEEE Robot Autom Lett 2020;5:1366–72.

[98] Alambeigi F, Sefati S, Armand M. A convex optimization framework for constrained concurrent motion control of a hybrid redundant surgical system. In: 2018 annual American control conference (ACC); 2018.

[99] Alambeigi F, Bakhtiarinejad M, Sefati S, Hegeman R, Iordachita I, Khanuja H, Armand M. On the use of a continuum manipulator and a bendable medical screw for minimally invasive interventions in orthopedic surgery. IEEE Trans Med Robot Bionics 2019;1:14–21.